Macromolecules

Article

pubs.acs.org/Macromolecules

Signatures of Intracrystallite and Intercrystallite Limitations of Charge Transport in Polythiophenes

Kiarash Vakhshouri,[†] Brandon H. Smith,[†] Edwin P. Chan,[§] Chenchen Wang,[∥] Alberto Salleo,[∥] Cheng Wang,[⊥] Alexander Hexemer,[⊥] and Enrique D. Gomez*[,†,‡]

[†]Department of Chemical Engineering and [‡]Materials Research Institute, Pennsylvania State University, University Park, Pennsylvania 16802, United States

[§]Polymers Division, National Institute of Standards and Technology, Gaithersburg, Maryland 20899, United States

[∥]Materials Science and Engineering, Stanford University, Stanford, California 94305, United States

[⊥]Advanced Light Source, Lawrence Berkeley National Laboratory, Berkeley, California 94530, United States

Supporting Information

ABSTRACT: Charge carrier mobilities in conjugated semicrystalline polymers depend on morphological parameters such as crystallinity, crystal orientation, and connectivity between ordered regions. Despite recent progress in the development of conducting polymers, the complex interplay between the aforementioned parameters and their impact on charge transport is not fully understood. By varying the casting solvents and thermal annealing, we have systematically modulated the crystallization of poly(3-hexylthiophene-2,5-diyl) (P3HT) and poly[2,5-bis(3-hexadecylthiophen-2-yl)thieno(3,2-*b*)thiophene] (PBTTT) thin films to examine the role of microstructure on charge mobilities. In particular, we achieve equal crystallinities through different processing routes to examine the role of structural parameters beyond the crystallinity on charge mobilities. As expected, a universal relationship does not exist between the crystallinity in either P3HT and PBTTT active layers and the charge mobility in devices. In P3HT films, higher boiling point solvents yield longer conjugation lengths, an indicator of stronger intracrystalline order, and therefore higher device mobilities. In contrast, the charge mobilities of PBTTT devices depend on the interconnectivity between crystallites and intercrystalline order in the active layer.

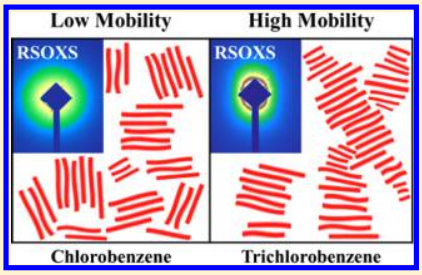

INTRODUCTION

Recent progress on the development of conjugated polymer semiconductors is driven by an emerging interest in flexible electronic devices for a myriad of applications ranging from complex displays to simple RFID tags.[1,2] Soluble polymers such as poly(3-hexylthiophene) (P3HT) and poly[2,5-bis(3-hexadecylthiophen-2-yl)thieno(3,2-*b*)thiophene] (PBTTT) exhibit an exclusive combination of optoelectronic properties, modest charge mobility, mechanical flexibility, and the potential for convenient, low cost, solution-based fabrication techniques (e.g., inkjet printing, roll-to-roll printing, etc.).[3−10] A variety of organic electronic devices are possible, such as light-emitting diodes, field-effect transistors, and photovoltaic cells, provided limitations in stability, performance, and reproducibility can be addressed. Part of the challenge is found in the lack of fundamental knowledge regarding the key factors that govern charge transport. Consequently, a critical challenge facing the implementation of polymeric semiconductors for digital electronics lies in understanding the role of the microstructure on the macroscopic electrical properties.

Charge transport within conjugated polymers occurs through polymer chain backbones (intrachain transport) and between different chains (interchain transport) due to electronic coupling between rings, such as through $\pi-\pi$ stacking.[11−13] The semicrystalline nature of many conjugated polymers creates a complex multiscale structure where not only the unit cell and disorder within crystals but other morphological parameters such as the crystallinity, orientation of the crystals, and connectivity between crystallites also affect transport.[14−20] Prior studies have observed that chain properties, including molecular mass, can alter the performance of conjugated Polymer thin film transistors by influencing structural parameters of the active layer.[21−24] For instance, low molecular mass (M_W < 4 kDa) P3HT films are highly crystalline but exhibit low charge mobilities in thin-film transistors.[25,26] High molecular mass films (M_W > 30 kDa) are less crystalline but yield higher carrier mobilities when used as the active layer in transistors. The inverse correlation between crystallinity and charge mobility implies that the crystallinity is not always the dominating morphological factor, despite the intuitive advantage of strong local order. Instead, the dependence of device mobilities on the molecular mass of the active layer suggests that interconnectivity can be a limiting factor for macroscopic charge transport because higher molecular mass polymers are expected to have more tie chains connecting crystallites.

Received: May 21, 2016
Revised: August 14, 2016
Published: September 20, 2016

DOI: 10.1021/acs.macromol.6b01086
Macromolecules 2016, 49, 7359−7369

Prior work has demonstrated that the crystallization kinetics of P3HT and PBTTT can affect the microstructure formation and crystallite interconnectivity, as rapid crystallization in polythiophenes leads to a higher density of tie chains bridging amorphous regions and connecting crystal domains.[27] Interconnectivity between crystallites in polymers is often characterized by measuring the elastic modulus (E), which above the glass transition temperature is linearly proportional to the number of tie chains per unit volume (ν) times kT plus the entanglement modulus (E_e), if tie chains are Gaussian, such that[28−31]

$$E = \nu kT + E_e \quad (1)$$

Smith, Heeger, and co-workers have measured the modulus of doped polyacetylene films and determined that the electrical conductivity increases with modulus and tensile strength.[23,24,32] In order to characterize the elastic modulus for thin-film geometries, a methodology has been developed that is based on measurements of internal stress obtained from observations of buckling due to mechanical compression.[33−36] Using this buckling technique, a correlation between the elastic modulus of various conjugated polymer films and the hole mobility of the polymer in devices was found.[37] Nevertheless, differences in the modulus (and effective tie chain density) will be strongly affected by the crystallinity of different polymers, thus confounding the relationship between moduli of active layers and charge mobilities in devices.[38−40]

Molecular orientation and alignment of the polymer backbones have also been reported to enhance charge transport through semicrystalline polymer thin films.[9,16,41−44] In one example, the mobility of poly(9,9′-dioctylfluorene-*co*-bithiophene) in devices increases by aligning the chains parallel to the transport direction in a nematic state.[42] Directional crystallization can also affect the charge mobilities in P3HT and PBTTT for devices fabricated parallel versus perpendicular to the crystallization growth direction of the active layer. The observed anisotropy in the extracted mobilities was attributed to stronger electrical percolation along the fibrils compared with percolation perpendicular to the fibrils due to larger barriers for charge transport at fibril-to-fibril grain boundaries.[16]

In the present work, we characterize structural parameters beyond the degree of crystallinity that can modulate charge transport in P3HT and PBTTT active layers, and we explore the correlations of each with observed organic thin-film transistor (OTFT) carrier mobilities. The degree of crystallinity in each sample was systematically controlled by changing the thermal annealing time and casting solvents during processing, and we compare P3HT and PBTTT films that exhibit the same relative crystallinity with different processing histories. An aggregation model was employed to ascertain conjugation lengths from UV−vis absorbance spectroscopy, and a buckling model allowed film modulus data and relative tie chain densities to be determined. Polarized soft X-ray scattering (RSOXS) methods were also applied to relate mechanical properties and orientational order to charge mobility.

MATERIALS AND METHODS

Solutions of poly(3-hexylthiophene) (P3HT) (96% H−T regioregular, M_n = 25 kg/mol, dispersity = 2.0, Merck[45]) and poly[2,5-bis(3-hexadecylthiophen-2-yl)thieno(3,2-*b*)thiophene] (PBTTT) (M_n = 26 kg/mol, dispersity = 1.9, Merck) were prepared with anhydrous chlorobenzene (CB) and 1,2,4-trichlorobenzene (TCB) (Sigma-Aldrich) in a nitrogen-purged glovebox. Solutions were stirred for a minimum of 12 h and heated to 90 °C for 1 and 5 min, respectively, prior to deposition to ensure complete dissolution. Films were spin-cast from 10 mg/mL hot solution (90 °C) at 1000 rpm for 1 min for solutions made with chlorobenzene. In the case of TCB, the solution was allowed to cool to room temperature, and films were spun at 1000 rpm for 3 min to obtain more uniform films.

Bottom-gate, bottom-contact field-effect transistors were fabricated using boron-doped p-type silicon wafers for the gate electrodes with a 300 nm thick thermally grown SiO_2 layer as the gate dielectric (C = 10.6 nF/cm^2, Process Specialties). Surface treatments were not applied to the dielectric surface to prevent film dewetting for some of the processing conditions employed in the study despite the lower overall charge mobilities generally observed for untreated devices.[27,46] Wafers were cleaned with acetone in an ultrasonic bath for 20 min followed by an additional 20 min of sonication in isopropanol. Gold source and drain electrodes approximately 100 nm thick were deposited using conventional double-layer photolithography to achieve channel widths of 220 μm and lengths of 20 μm. In order to study the effect of annealing time, fabricated devices were annealed on a calibrated digital hot plate at 150 °C for various lengths of time. All dissolution, spin-casting, thermal annealing, and electrical testing was performed in a nitrogen-purged glovebox without exposing the devices to air.

UV−vis spectroscopic measurements were completed with a Beckman DU Series 500 spectrophotometer for films spin coated onto glass substrates (Eagle XG, Corning Incorporated, Glass Dynamics). All spectra are normalized to the highest polymer absorption peak. Atomic force microscopy (AFM) experiments were performed using a Bruker Dimension Icon instrument. AFM topography and phase images were recorded simultaneously in tapping mode with the driving frequency set equal to the resonant frequency of the probe in the immediate vicinity of the sample surface.

For buckling measurements, as-deposited PBTTT thin films were peeled off silicon substrates and supported by a 2 mm thick polydimethylsiloxane (PDMS) layer. The PDMS film was cast with a cross-linker concentration of 10:1 and cured at a temperature of 50 °C for over 12 h. The elastic modulus of PDMS was measured with a texture analyzer (Texture Technologies TX.XT2i) employing a tensile test procedure. The reported buckling wavelength was based on a count of the number of buckles observed in a row of specified length. The row length was then divided by the number of buckling events, and the average value was reported as the characteristic wavelength.

X-ray diffraction (XRD) experiments were undertaken to measure the relative crystallinity of thin polymer films. Silicon (100) wafer substrates (Silicon Sense) were cleaned thoroughly by sonicating in acetone and isopropanol for 20 min each and scouring the surface with UV−O_3 for 10 min. Diffraction measurements were performed at the Pennsylvania State University Material Characterization Laboratory using a Rigaku DMAX-Rapid microdiffractometer with a 2-dimensional curved image plate detector and copper Kα X-rays (λ = 1.54 Å). Rocking curves were obtained by tilting the sample (±0.2°) around the (100) peak for P3HT and the (200) peak for PBTTT during data acquisition. Intensities were obtained as a function of azimuthal angle by integrating over a q = ±0.019 Å^{-1} scattering vector window ($q = 4\pi \sin(\theta/2)/\lambda$). A linear background was subtracted from the rocking curve data using intensities away from the Bragg peak of interest. Crystallinities were measured by azimuthally integrating the (100) or (200) reflection obtained from the rocking scan. The values were corrected for differences in thickness between films cast from different solvents and normalized to the highest relative crystallinity observed.

Thin films of P3HT and PBTTT for polarized resonant soft X-ray scattering (RSOXS) experiments were spin-cast from 10 mg/mL solutions of chlorobenzene and 1,2,4-trichlorobenzene onto roughly 65 nm thick layers of poly(3,4-ethylenedioxythiophene):poly(styrenesulfonate) (PEDOT:PSS) (Clevios P, H.C. Starck) deposited on silicon wafers. Silicon wafers were precleaned by sonicating for 20 min in acetone and isopropanol, followed by 10 min of ultraviolet light ozonation. As-cast films were subsequently floated in ultrapure deionized water (18.2 MΩ/cm) and caught with 5 mm × 5 mm silicon frames supporting a 1 mm × 1 mm × 100 nm Si_3N_4 window. Samples were dried for 24 h under vacuum at room temperature and

DOI: 10.1021/acs.macromol.6b01086
Macromolecules 2016, 49, 7359−7369

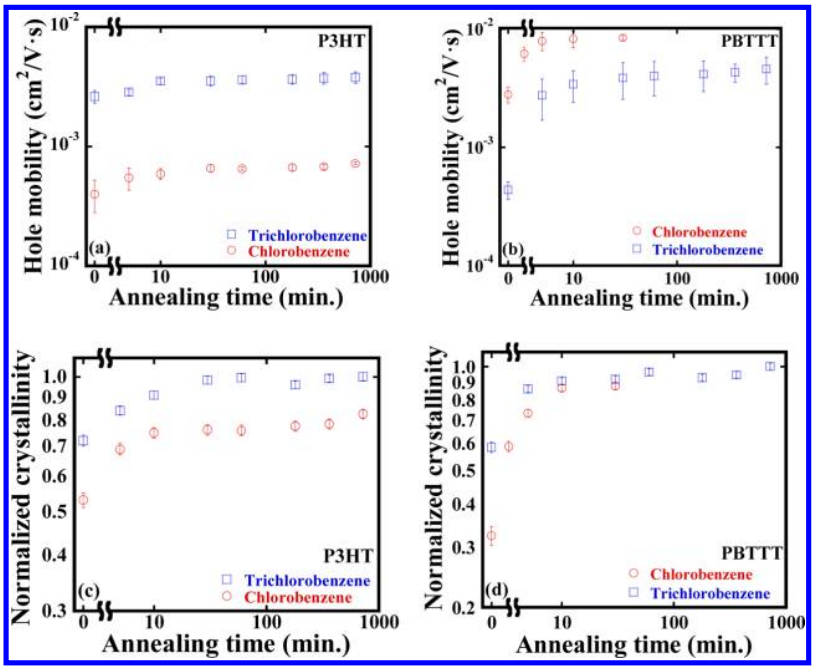

Figure 1. Effect of annealing time on relative crystallinity and mobility for (a, c) P3HT and (b, d) PBTTT thin films spun-cast from chlorobenzene and 1,2,4-trichlorobenzene. Samples were annealed at 150 °C.

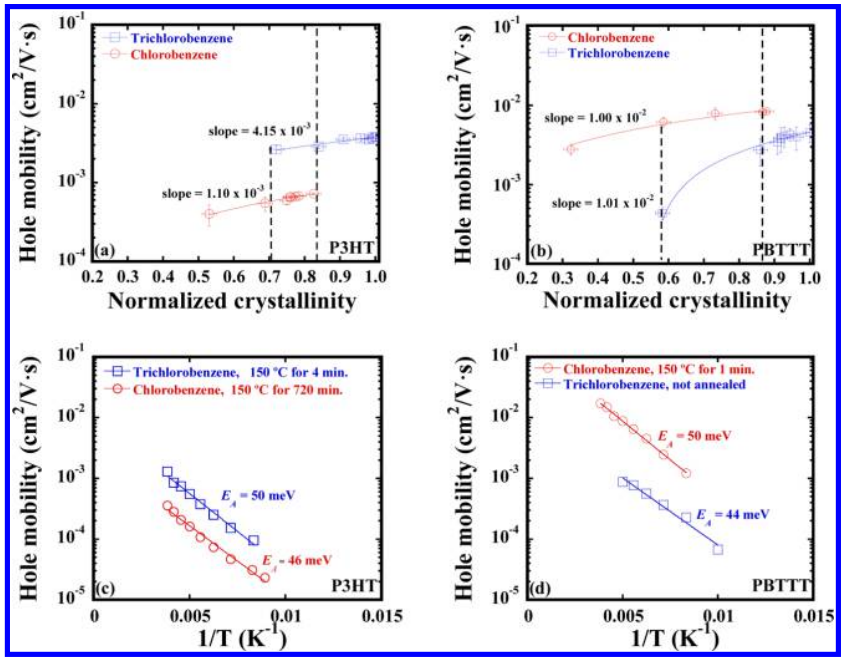

Figure 2. Comparison of the mobility and crystallinity for (a) P3HT and (b) PBTTT thin films. Solid lines are linear fits to the data, and dashed lines highlight samples with the same degree of crystallinity. Temperature-dependent mobility of (c) P3HT and (d) PBTTT films with the same relative degree of crystallinity, 0.83 and 0.58, respectively. Samples were annealed at 150 °C for various annealing times. Lines in (c) and (d) indicate exponential fits to the data.

annealed on a calibrated digital hot plate in a nitrogen-purged glovebox. RSOXS measurements were conducted in the transmission geometry in vacuum at Beamline 11.0.1 of the Advanced Light Source at Lawrence Berkeley National Laboratory. Detector images were azimuthally or radially integrated as a function of the scattering vector, and dark image background noise and scattering from the silicon nitride window were subtracted from the data. Anisotropic scattering patterns were obtained with linear horizontally and vertically polarized photons at an energy of 285.4 eV.

RESULTS AND DISCUSSION

The field-effect mobility of P3HT and PBTTT active layers was probed by fabricating bottom-contact, bottom-gate thin-film transistors from chlorobenzene and 1,2,4-trichlorobenzene solutions. To avoid dewetting issues over the large range of processing parameters used in this study, no surface treatments (i.e., self-assembled monolayers) were applied during device fabrication, leading to lower charge mobilities than previously

DOI: 10.1021/acs.macromol.6b01086
Macromolecules 2016, 49, 7359−7369

reported.[27,46] Nevertheless, similar trends were observed when a trimethoxy(octadecyl)silane SAM layer was incorporated. (see Figures S1 and S2 in the Supporting Information). Samples were annealed at 150 °C for increasing lengths of time, and extracted mobility values are shown in Figure 1. P3HT films cast from 1,2,4-trichlorobenzene displayed much higher performance than those cast from chlorobenzene, but the reverse was true for PBTTT films. Hole mobilities increased rapidly with annealing time up to 10 min for all samples and slowly after 10 min. The effect of annealing on charge mobilities is likely due to changes in microstructure, but the specific aspect of the microstructure that dominates charge transport must be identified.[47,48]

One aspect that likely affects charge mobilities is the degree of crystallinity. The relative crystallinity of each sample was estimated from azimuthal integrations of X-ray diffraction intensities at the P3HT (100) and PBTTT (200) reflections obtained from rocking scans.[27,49] The values of the crystallinity were normalized by film thickness to account for variations imparted by the different boiling points of the two solvents. Thus, we estimate the relative crystallinity of the entire film, even though transport in organic thin-film transistors is localized to a few nanometers next to the dielectric surface.[50−52] The crystallinity of the whole film is expected to roughly track the crystallinity near the bottom surface because the bottom surface nucleates crystals within the film and leads to highly textured crystalline films.[53] As observed for charge mobility, the relative crystallinity, shown as a function of annealing time in Figure 1, increases rapidly prior to 10 min and levels off. Nevertheless, the crystallinities of PBTTT films from chlorobenzene or 1,2,4-trichlorobenzene converge at long annealing times whereas the mobility values never converge. As expected, the relative crystallinity alone cannot explain the deviations between the two solvent systems. The crystal orientation (crystalline texture) and coherence lengths from the (100) and (010) reflections are shown in Figures S3−S6 for the various P3HT and PBTTT films. None of these track with the mobility.

Although the mobility tracks the relative crystallinity for samples cast from a single solvent, the curves are unmistakably offset for different solvents. Nevertheless, samples with equal crystallinities were studied to identify how much of this difference is due to the crystallinity. In Figure 2, the charge carrier mobility is plotted against the normalized crystallinity. The dashed lines in Figure 2a confirm that at the same degree of crystallinity the charge mobilities of P3HT samples spin-cast from 1,2,4-trichlorobenzene are higher. Likewise, dashed lines in Figure 2b indicate PBTTT samples with the same crystallinity, but hole mobilities are significantly higher when active layers are cast from chlorobenzene instead of 1,2,4-trichlorobenezene.

Characterization of the temperature-dependent mobility enables further scrutiny of charge transport in films with equal crystallinities but disparate mobilities. As shown in Figures 2c and 2d, hole mobilities were measured as a function of temperature for P3HT and PBTTT thin films possessing the same degree of relative crystallinity (dashed lines in Figures 2a and 2b). P3HT films were cast from chlorobenzene and 1,2,4-trichlorobenzene and annealed at 150 °C for 720 and 4 min, respectively, to achieve comparable crystallinities. Similarly, PBTTT films were analyzed as-cast and after annealing at 150 °C for 1 min, where the two films exhibit similar crystallinities, coherence lengths, and crystallite texture (Figures S3 and S4). The increase in charge mobilities with increasing temperature can be attributed to thermally activated transport, which is commonly observed in organic semiconductors.[54,55] Although mobility values from each solvent system are consistently different for both polymers, the temperature dependence and, consequently, the activation energies (E_A) remain unchanged. This suggests that the dominant phenomena that leads to activated transport, namely charge hopping events, are unaffected by the casting solvent. Instead, the number of percolating pathways for transport must vary between samples cast from different solvents.

The absorption spectrum provides significant insights into the molecular order, geometry, and local environment of conjugated molecules.[7] As such, much effort has been applied toward interpreting the absorption and emission spectra of polymer films in terms of microstructure and morphology.[56−62] Lower energy features in the absorption spectrum of highly ordered polymers like regioregular P3HT are usually attributed to interchain coupling leading to delocalization of the excitation across multiple chains, while higher energy features are ascribed to excitons localized to single chains.[60] Therefore, the presence of interchain excitons is interpreted as an identifier that some local ordering allows charge delocalization across π-stacked chains within P3HT films.[63]

In a model developed by Spano, a quantitative analysis was proposed for regioregular P3HT absorption spectra to extract morphological parameters such as conjugation length. The model is based on weakly coupled H-aggregates of P3HT chains (parallel-aligned and cofacially packed) where the splitting of the electronic levels from Coulombic interactions is smaller than the vibrational energy. An excitonic band with bandwidth W will form due to these interchain interactions, which is related to the strength of the intermolecular coupling in the $\pi-\pi$ stacking direction.[59,64,65] According to the model, the exciton bandwidth can be estimated from the ratio of the 0−0 to the 0−1 vibronic peaks, and prior work involving quantum-chemical calculations has demonstrated that W decreases with increasing conjugation length.[66,67] W, and by inference, the conjugation length of P3HT, can therefore be estimated from the absorption spectra of thin films using Spano's model.

Figure 3 depicts the UV−vis absorption spectra for two P3HT films with the same degree of relative crystallinity. The model was applied to deconvolute the contributions from aggregated and amorphous regions of the thin films. Five Gaussian vibronic peaks were used to fit the aggregated portion of the spectra and estimate W for each sample. For films spin-cast from chlorobenzene and 1,2,4-trichlorobenzene, W was found to be 94 and 55 meV, respectively, suggesting that processing films from 1,2,4-trichlorobenzene generates longer conjugation lengths. The higher mobilities observed in devices prepared from 1,2,4-trichlorobenzene can therefore be attributed to the longer intramolecular conjugation length that developed despite equivalent crystallinities in the active layer.

Similar analyses were also performed on absorption spectra of P3HT films annealed for increasing lengths of time to further probe the effect of conjugation length on charge mobility. The results, provided in Figure 3c, demonstrate that thermal annealing decreases the exciton bandwidth and increases the conjugation length. More importantly, the data illustrate that all thin films cast from 1,2,4-trichlorobenzene exhibit lower W values than films spun from chlorobenzene, suggesting that in

DOI: 10.1021/acs.macromol.6b01086
Macromolecules 2016, 49, 7359−7369

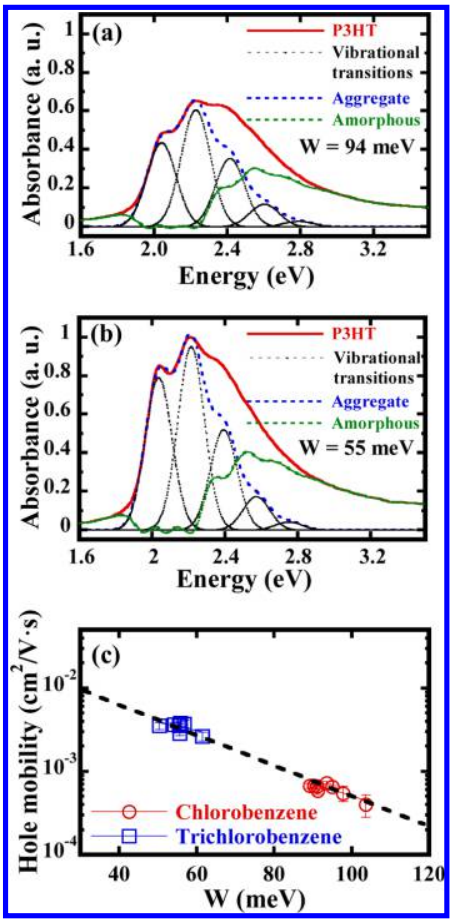

Figure 3. Experimental and simulated absorption spectra measured at room temperature for P3HT films spun from (a) chlorobenzene, annealed at 150 °C for 720 min, and (b) 1,2,4-trichlorobenzene, annealed at 150 °C for 4 min. Both samples have the same degree of crystallinity. (c) Mobility as a function of free exciton bandwidth for P3HT films spin-cast from chlorobenzene and 1,2,4-trichlorobenzene. Data points represent various annealing times.

addition to crystallinity other parameters such as conjugation length can modulate the charge carrier mobility. Studies focusing on organic solar cells also provide corroborative evidence, reporting that casting from high boiling point solvents often yields longer conjugation lengths and more efficient photovoltaic performance.[68−70]

The spectroscopic signatures of changes in the conjugation length suggest changes in the backbone chain conformation and orientation. Poor sensitivity and spatial resolution in organic films often require the application of a suite of optical, X-ray, and electron microscopy analysis methods to survey the orientation of crystallites.[7,71−76] Because of the excellent sensitivity toward bond orientation provided by polarized resonant soft X-ray scattering (RSOXS), this technique has recently proved useful for probing noncrystalline orientational organization in thin films with high resolution.[44] At the resonant energy for anisotropic orbitals (C 1s → $\pi^*_{C=C}$, 285.4 eV), the orientation contrast is higher than mass−thickness contrast, so RSOXS can reveal noncrystalline orientational ordering in organic thin films and molecular orientational information from scattering anisotropy. In this study, RSOXS for two perpendicular photon electric fields at the resonant energy was utilized to unravel the molecular orientation differences between two samples with the same degree of crystallinity for both P3HT and PBTTT.

Figure 4 shows the scattering patterns obtained using linear horizontal and vertical polarization for P3HT thin films spun

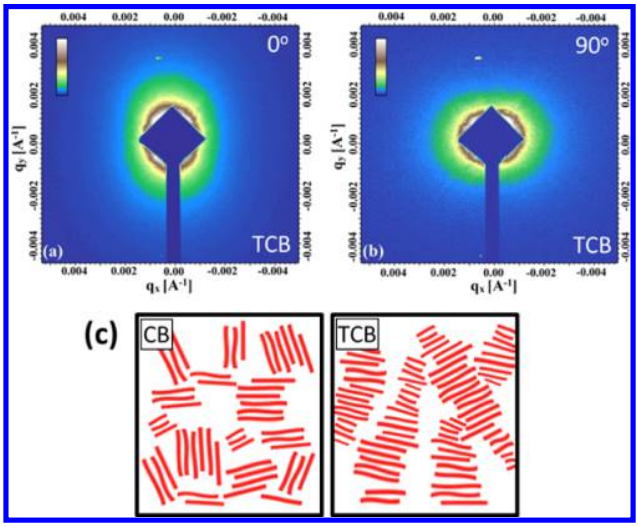

Figure 4. Anisotropic RSOXS patterns obtained using linear (a) horizontally and (b) vertically polarized photons at an energy of 285.4 eV for a thin P3HT film spin-cast from 1,2,4-trichlorobenzene and annealed at 150 °C for 4 min. The linear intensity scale bar is in arbitrary units. Schematic of the fibril microstructure of P3HT cast from (c) chlorobenzene (CB) and (d) 1,2,4-trichlorobenzene (TCB), showing the longer fibrils in films cast from 1,2,4-trichlorobenzene that lead to anisotropic soft X-ray scattering. Backbones are shown as lines in (c) and (d), and amorphous chains are not shown.

cast from 1,2,4-trichlorobenzene and annealed at 150 °C for 4 min. The scattering between the two polarizations is anisotropic with higher intensities along certain azimuthal directions. It is also independent of sample rotation, demonstrating no global preferential alignment within the sample. This is remarkable because anisotropic scattering has not been previously reported for thin films spun cast from a neat homopolymer. Collins and co-workers have reported anisotropic scattering for blends of P3HT and poly([*N*,*N*′-bis(2-octyldodecyl)-11-naphthalene-1,4,5,8-bis(dicarboximide)-2,6-diyl]-*alt*-5,5′-(2,2′-12-biothiopene)) P(NDI20D-T2), and attributed the anisotropy to highly aligned P(NDI2OD-T2) molecules at the interface between the two materials with π orbitals pointed toward the boundary.[44] Analogously, we surmise that the anisotropic scattering observed in neat P3HT (Figure 4) is due to local correlations between chain backbones within the thin film.

Average scattering profiles for P3HT thin films exhibiting equal crystallinity spun from 1,2,4-trichlorobenzene and chlorobenzene solutions and annealed at 150 °C for 4 and 720 min, respectively, are included in Figure 5 for the q range between 0.012 and 0.0012 Å^{-1}. At large q, data for films cast from 1,2,4-trichlorobenzene and chlorobenzene both scale with q^{-2}, suggesting scattering dominated by chain-like objects (Debye scattering).[77] Alternatively, scattering could be from 2D objects, but because q^{-1} exceeds or is near the film thickness, q^{-2} scaling is not expected.[78]

Fitting the scattering data to the Debye function suggests radii of gyration of 82 nm for films cast from chlorobenzene and greater than about 150 nm for films cast from 1,2,4-

DOI: 10.1021/acs.macromol.6b01086
Macromolecules 2016, 49, 7359−7369

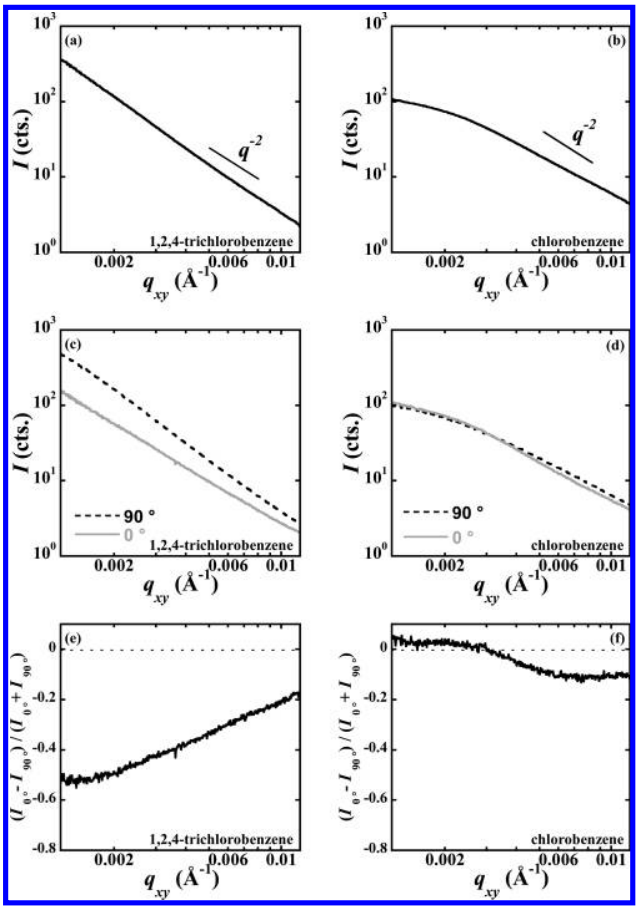

Figure 5. RSOXS profiles for thin P3HT films spun cast from (a) 1,2,4-trichlorobenzene and annealed at 150 °C for 4 min and (b) chlorobenzene annealed at 150 °C for 720 min. (c, d) Corresponding scattering profiles at 0° (horizontal CCD direction) and 90° (vertical CCD direction) obtained with linear horizontally polarized photons at an energy of 285.4 eV. (e, f) Corresponding anisotropy ratio of intensities from radial scattering profiles at 0 and 90°.

trichlorobenzene. These dimensions are much larger than the radius of gyration of chains, which we expect to be about 8 nm with a persistence length of 3 nm and molecular mass of 25 kg/mol.[77,79,80] Instead, we attribute the scattering contrast within P3HT to the fibril-like crystallites and the amorphous matrix. Previous TEM and AFM images suggest that P3HT fibrils can bend as worm-like objects.[81−85] Thus, fibrils are more extended when films are cast from 1,2,4-trichlorobenzene than chlorobenzene, implying that anisotropy within RSOXS data should differ between films cast from 1,2,4-trichlorobenzene and chlorobenzene.

Corresponding radial scattering profiles with 60° sector widths obtained from 0° and 90° linear horizontally polarized photons are also shown in Figure 5. Large differences between scattering data at 0° and 90°, especially at low q, are apparent between the profiles for films cast from 1,2,4-trichlorobenzene, whereas samples prepared from chlorobenzene demonstrate no clear differences between profiles. The anisotropy ratio, which is calculated from the difference in scattering intensity between 0° and 90°, confirms the clear anisotropy for the film from 1,2,4-trichlorobenzene but shows little anisotropy for the chlorobenzene sample at low q. The anisotropy visible in RSOXS P3HT data suggests that thin films cast from 1,2,4-trichlorobenzene and chlorobenzene develop different morphologies and molecular orientation even though the samples possess the same degree of crystallinity.

Although anisotropy in RSOXS data is not yet fully understood, we hypothesize that anisotropic scattering is a result of correlations between the orientation of chain backbones in adjacent domains. Electronic transitions have dipole moments along specific directions due to the fact that molecular orbitals can be anisotropic, and as a result, the transitions will be sensitive to the direction of the photon electric field.[86,87] In the C 1s → $\pi^*_{C=C}$ transition at a resonant energy of 285.4 eV, only those π orbitals aligned with the photon electric field contribute to the scattering observed from RSOXS. Nevertheless, even if molecular orbitals are aligned within domains but these domains are randomly oriented, then isotropic scattering should occur. One origin of anisotropy is correlations in orientation between domains because that would suppress scattering in the direction perpendicular to the molecular orbitals when linearly polarized X-rays are used. Here we take anisotropy as a result of contrast in molecular order (backbone orientation) between crystalline and amorphous regions in P3HT films. Thus, we surmise that P3HT thin films with short crystalline fibrils show no anisotropy due to the isotropic and random distribution of short P3HT fibrils in the amorphous domains.

On the other hand, in films with long P3HT crystalline fibrils, contrast between the fibrils aligned with the electric field and amorphous regions will be pronounced only in certain directions, resulting in anisotropic scattering patterns. In other words, the anisotropic shape of long fibrils, the packing of these fibrils at distances shorter than the length of the fibril, and the perpendicular alignment of P3HT backbones (and π orbitals) with respect to the fibril direction lead to RSOXS scattering that is anisotropic in azimuthal angle (Figure 4c). Thus, casting P3HT thin films from 1,2,4-trichlorobenzene could result in longer crystalline fibrils that cause the anisotropy observed with RSOXS. As shown in Figure S7, P3HT films cast from 1,2,4-trichlorobenzene show stronger evidence of long, well-defined fibrils in AFM images. The longer fibrils do not lead to a significant increase in the π-stacking coherence length because the (010) peak width measured by X-ray diffraction is limited by thermal fluctuations and cumulative disorder.[88] Another explanation is that order within the crystallites is stronger in films cast from 1,2,4-trichlorobenzene, such that the chain backbones are more aligned perpendicular to the long fibril axis. This is consistent with the longer conjugation lengths that are apparent from the absorption spectra because the more aligned backbones are presumably within crystallites and they imply fewer torsional kinks along the chains.

We hypothesize that intracrystallite order in P3HT is critical for charge transport when the molecular mass of P3HT is high, such that interconnectivity between crystallites is established through tie chains. Longer conjugation lengths, stronger orientational order, and better defined fibrils are all morphological signatures that suggest improved charge transport. For PBTTT, the absorption spectra are not significantly different for the two sets of samples with the same crystallinity identified in Figure 2b. Furthermore, RSOXS shows no evidence of scattering anisotropy (see Figures S8 and S9). We therefore examine signatures of interconnectivity between crystallites for high molecular mass PBTTT.

As with P3HT, hypotheses that other parameters besides crystallinity and orientational order, e.g. crystallite interconnec-

DOI: 10.1021/acs.macromol.6b01086
Macromolecules 2016, 49, 7359−7369

tivity, can regulate the charge carrier mobility in PBTTT thin films have been suggested.[25−27] Interconnectivity within ordered regions of semicrystalline polymer films is related to the number of tie chains connecting distinct crystallites. Orientational correlations between crystallites are likely indicative of interconnectivity by tie chains because preserving orientational order probably requires connetions between adjacent crystals and because chains may be more likely to bridge crystallites if significant backbone deflections are not required, especially if chains are stiff. Collins et al. demonstrated that RSOXS can be used to measure the average length over which the polymer backbones are aligned with each other. For example, RSOXS could be sensitive to the spacing between domains with the same texture because face-on crystallites will have much lower absorption at the 1s → π^* edge and therefore provide contrast when compared to edge-on crystals. The average correlation length is taken as half of the spacing measured by features or peaks in RSOXS profiles, and this length scale in PBTTT active layers is directly correlated to charge carrier mobilities in thin-film transistors.[44]

RSOXS scattering profiles for PBTTT thin films cast from chlorobenzene and 1,2,4-trichlorobenzene are compared in Figure 6. Features or shoulders in the scattering near q = 0.002

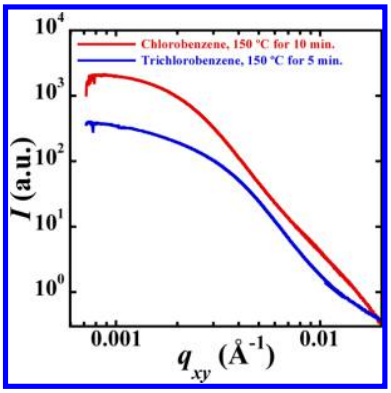

Figure 6. RSOXS scattering profiles at 285.4 eV of PBTTT thin films spun from chlorobenzene and 1,2,4-trichlorobenzene and annealed at 150 °C for 10 and 5 min, respectively. Both samples exhibit the same degree of crystallinity.

Å^{-1} and 0.004 Å^{-1} are apparent in the chlorobenzene and 1,2,4-trichlorobenzene films, respectively, and are also apparent as peaks when plotted as Iq^2 (see **Figure S10** of the Supporting Information). The orientational correlation length for samples spun cast from chlorobenzene and annealed at 150 °C for 10 min is approximately 160 nm. In contrast, the orientational correlation length for films cast from 1,2,4-trichlorobenzene and annealed at 150 °C for 5 min is roughly 80 nm. The higher charge carrier mobility extracted for PBTTT cast from chlorobenzene is correlated to the higher orientational correlation length achieved in the film, and perhaps to a higher density of tie chains.

Previous studies have employed rheology experiments to measure the elastic modulus of bulk samples and estimated the number of tie chains.[28,29] If tie chains have Guassian conformations, the modulus is the sum of contribution from entanglements and tie chains; otherwise, corrections exist to account for tie chain stretching (eq 1).[89−93] Thus, we measured the elastic modulus of PBTTT films and compared them to carrier mobilities of devices under the assumption that the modulus is proportional to tie chain densities. Estimates of the modulus for film samples were ascertained using a technique in which an internal stress measurement is made by analyzing buckling phenomena during mechanical compression.[33,34] The elastic modulus is obtained from the buckling wavelength measured by optical microscopy using eq 2, where λ is the wavelength of the buckling, h is the film thickness, and E is the elastic modulus.[94,95] The subscripts "f" and "s" denote film and substrate.

$$\bar{E}_f = 3\bar{E}_s\left(\frac{\lambda}{2\pi h}\right)^3 \quad (2)$$

Figure 7 shows the moduli of PBTTT thin films as a function of strain for samples spun from chlorobenzene and 1,2,4-

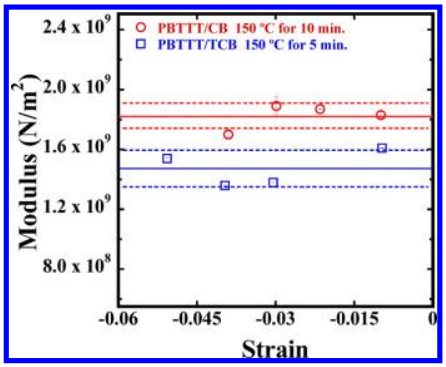

Figure 7. Thin film moduli of PBTTT films spun-cast from chlorobenzene and 1,2,4-trichlorobenzene and annealed at 150 °C for 10 and 5 min, respectively. Both sets of samples have the same degree of crystallinity. Solid lines represent the average modulus for each case, and dashed lines represent standard deviations.

trichlorobenzene annealed at 150 °C for 10 and 5 min, respectively. The annealing conditions were chosen to ensure that both samples exhibited the same degree of crystallinity as indicated by the dashed line in Figure 2. The average elastic modulus of films cast from chlorobenzene is 1.82 ± 0.08 GPa, and 1.47 ± 0.12 GPa is obtained for films spun from 1,2,4-trichlorobenzene. Previous measurements of the modulus of PBTTT thin films annealed at 180 °C for 5 min reported a value of 1.80 ± 0.34 GPa, which is in the same range as the moduli reported in this study.[37] PBTTT films with a higher moduli is indicative of a higher number of tie chains that provide more pathways for charge transport between crystallites and thus exhibit higher charge carrier mobilities when used as the active layer in devices. In contrast, the modulus of P3HT films is not correlated with charge mobilities in devices, as evident when comparing Figure 2 and Figure S11. Instead, the modulus is slightly lower for the P3HT film that exhibits higher charge mobilities when applied as the active layer in devices. Unfortunately, we cannot compare the moduli between P3HT and PBTTT to ascertain relative tie chain densities between the two materials because the modulus of semicrystalline polymers depends on both the entanglement modulus and tie chain density.

The fused thiophene rings in PBTTT have low conformational freedom leading to a relatively rigid polymer backbone.[40,96,97] We estimate the persistence length of PBTTT to be 4.1 nm using the freely rotating chain model, larger than that of P3HT (2.8 nm).[80] Accordingly, the sample possessing the larger number of tie chains is in principle expected to exhibit

DOI: 10.1021/acs.macromol.6b01086
Macromolecules 2016, 49, 7359−7369

higher orientational correlation lengths due to the stiffness of the polymer backbone. The combined data shown from Figures 6 and 7 indicate that PBTTT thin films cast from chlorobenzene develop a higher number of tie chains bridging crystallites and higher orientational correlation lengths.

A possible explanation for the greater tie chain density acquired from chlorobenzene compared to 1,2,4-trichlorobenzene may lie in the difference between the boiling points of each solvent. Casting from low boiling point solvents causes rapid evaporation of the solvent allowing only a short time for rearrangement of the polymer chains and promotion of entanglements and tie chains.[98,99] Higher charge mobilities of PBTTT thin films cast from chlorobenzene can therefore be attributed to higher orientational correlation lengths and tie chain density. Alternatively, chlorobenzene could be more effective at inducing liquid crystalline order in PBTTT than 1,2,4-trichlorobenzene, and liquid crystalline order in the active layer can enhance charge mobilities of devices.[40] But, the higher boiling point of 1,2,4-trichlorobenzene makes it more likely to promote liquid crystallinity because the solvent likely stays longer in the film during casting. Altogether, the results suggest that, in addition to the degree of crystallinity, charge transport in high molecular mass PBTTT depends on the interconnectivity between crystalline regions and extended orientational order.

CONCLUSIONS

The factors governing charge transport within P3HT and PBTTT have been systematically studied as a function of relative crystallinity by varying thermal annealing conditions and casting solvents. As expected, the results demonstrate that a universal correlation between crystallinity and mobility does not exist; other structural parameters must be considered. An aggregation model was employed to estimate the conjugation length and interchain interactions from absorption spectra of P3HT films, and longer conjugation lengths imparting higher charge mobility were obtained from higher boiling point solvents. Moreover, anisotropic scattering profiles indicative of longer or better ordered crystalline fibrils were observed from RSOXS measurements for P3HT films spin-cast from 1,2,4-trichlorobenzene that lead to higher charge mobilities in devices.

Similar studies of PBTTT films coupled with thin film modulus measurements suggest that the molecular orientation and tie chain interconnectivity can be correlated with mobility. The combined evidence demonstrates that the choice of solvent can alter the conjugation length and molecular orientation within crystallites in P3HT, which in turn affects charge transport, and the choice of solvent can also affect the orientational order and interconnectivity between crystalline regions that modulate the charge mobility in PBTTT. The thin-film moduli of P3HT films cast from 1,2,4-trichlorobenzene do not track the charge mobilities extracted from devices, suggesting that the intercrystalline connectivity is not responsible for the difference in charge mobilities between devices cast from either chlorobenzene or 1,2,4-trichlorobenzene. Instead, we hypothesize that intracrystalline order, as measured from conjugation lengths extracted from absorption spectra and anisotropic soft X-ray scattering, modulates charge mobilities in high molecular mass P3HT. In contrast, the orientational correlation length from RSOXS and thin-film moduli imply that PBTTT is limited by intercrystallite connectivity. We hypothesize that this difference between the two polymers is a consequence of the stiffer PBTTT chains (persistence length from the freely rotating chain model of 2.8 nm for P3HT and 4.1 nm for PBTTT[80]). Consequently, quantitative measurements of the elastic modulus and subsequent deductions from orientational order, mechanical properties, and charge transport correlations in thin conjugated polymer films can be implemented to guide the development of new high performance semiconductors for flexible organic electronics.

ASSOCIATED CONTENT

Supporting Information

The Supporting Information is available free of charge on the ACS Publications website at DOI: 10.1021/acs.macromol.6b01086.

A comparison of the transfer and output characteristics for PBTTT films on untreated and OTS treated SiO_2 substrates, atomic force microscopy (AFM) micrographs of P3HT thin films, RSOXS scattering patterns and radial scattering profiles for PBTTT films, plots demonstrating the effect of annealing time on crystal orientation and coherence length for P3HT and PBTTT films cast from 1,2,4-trichlorobenzene and chlorobenzene, and moduli results for P3HT films (PDF)

AUTHOR INFORMATION

Corresponding Author

*E-mail edg12@psu.edu (E.D.G.).

Notes

The authors declare no competing financial interest.

ACKNOWLEDGMENTS

Duc T. Duong is gratefully acknowledged for assistance in analyzing absorption spectra. Major funding for this work was provided by the Center for Flexible Electronics at Penn State sponsored by The Dow Chemical Company and NSF under Grant DMR-1056199. The authors also acknowledge the support of the Advanced Light Source, Lawrence Berkeley National Laboratory, which is supported by the U.S. Department of Energy under Contract DE-AC02-05CH11231.

REFERENCES

(1) Jackson, T. N.; Yen-Yi, L.; Gundlach, D. J.; Klauk, H. Organic thin-film transistors for organic light-emitting flat-panel display backplanes. *IEEE J. Sel. Top. Quantum Electron.* **1998**, *4*, 100−104.

(2) Cantatore, E.; Geuns, T. C. T.; Gelinck, G. H.; van Veenendaal, E.; Gruijthuijsen, A. F. A.; Schrijnemakers, L.; Drews, S.; de Leeuw, D. M. A 13.56-MHz RFID System Based on Organic Transponders. *IEEE J. Solid-State Circuits* **2007**, *42*, 84−92.

(3) Sirringhaus, H.; Kawase, T.; Friend, R. H.; Shimoda, T.; Inbasekaran, M.; Wu, W.; Woo, E. P. High-resolution inkjet printing of all-polymer transistor circuits. *Science* **2000**, *290*, 2123−2126.

(4) Sirringhaus, H.; Tessler, N.; Friend, R. H. Integrated Optoelectronic Devices Based on Conjugated Polymers. *Science* **1998**, *280*, 1741−1744.

(5) Bao, Z. Materials and Fabrication Needs for Low-Cost Organic Transistor Circuits. *Adv. Mater.* **2000**, *12*, 227−230.

(6) Brady, M. A.; Su, G. M.; Chabinyc, M. L. Recent progress in the morphology of bulk heterojunction photovoltaics. *Soft Matter* **2011**, *7*, 11065−11077.

(7) Salleo, A.; Kline, R. J.; DeLongchamp, D. M.; Chabinyc, M. L. Microstructural Characterization and Charge Transport in Thin Films of Conjugated Polymers. *Adv. Mater.* **2010**, *22*, 3812−3838.

DOI: 10.1021/acs.macromol.6b01086
Macromolecules 2016, 49, 7359−7369

(8) Forrest, S. R. The path to ubiquitous and low-cost organic electronic appliances on plastic. *Nature* **2004**, *428*, 911−918.
(9) Dyreklev, P.; Gustafsson, G.; Inganäs, O.; Stubb, H. Polymeric field effect transistors using oriented polymers. *Synth. Met.* **1993**, *57*, 4093−4098.
(10) Abdulrazzaq, O. A.; Saini, V.; Bourdo, S.; Dervishi, E.; Biris, A. S. Organic Solar Cells: A Review of Materials, Limitations, and Possibilities for Improvement. *Part. Sci. Technol.* **2013**, *31*, 427−442.
(11) Ehinger, K.; Roth, S. *Electronic Properties of Polymers and Related Compounds*; Solid State Sciences Series; Kuzmany, H., Mehring, M., Roth, S., Eds.; Springer-Verlag: Berlin, 1985.
(12) Bao, Z.; Locklin, J. J. *Organic Field-Effect Transistors*; CRC Press: Boca Raton, FL, 2007.
(13) Jaiswal, M.; Menon, R. Polymer electronic materials: a review of charge transport. *Polym. Int.* **2006**, *55*, 1371−1384.
(14) Kline, R. J.; McGehee, M. D. Morphology and Charge Transport in Conjugated Polymers. *J. Macromol. Sci., Polym. Rev.* **2006**, *46*, 27−45.
(15) Sirringhaus, H.; Brown, P. J.; Friend, R. H.; Nielsen, M. M.; Bechgaard, K.; Langeveld-Voss, B. M. W.; Spiering, A. J. H.; Janssen, R. A. J.; Meijer, E. W.; Herwig, P.; de Leeuw, D. M. Two-dimensional charge transport in self-organized, high-mobility conjugated polymers. *Nature* **1999**, *401*, 685−688.
(16) Jimison, L. H.; Toney, M. F.; McCulloch, I.; Heeney, M.; Salleo, A. Charge-Transport Anisotropy Due to Grain Boundaries in Directionally Crystallized Thin Films of Regioregular Poly(3-hexylthiophene). *Adv. Mater.* **2009**, *21*, 1568−1572.
(17) Lee, M. J.; Gupta, D.; Zhao, N.; Heeney, M.; McCulloch, I.; Sirringhaus, H. Anisotropy of Charge Transport in a Uniaxially Aligned and Chain-Extended, High-Mobility, Conjugated Polymer Semiconductor. *Adv. Funct. Mater.* **2011**, *21*, 932−940.
(18) Rivnay, J.; Jimison, L. H.; Northrup, J. E.; Toney, M. F.; Noriega, R.; Lu, S.; Marks, T. J.; Facchetti, A.; Salleo, A. Large modulation of carrier transport by grain-boundary molecular packing and microstructure in organic thin films. *Nat. Mater.* **2009**, *8*, 952−958.
(19) Jimison, L. H.; Salleo, A.; Chabinyc, M. L.; Bernstein, D. P.; Toney, M. F. Correlating the microstructure of thin films of poly[5,5-bis(3-dodecyl-2-thienyl)-2,2-bithiophene] with charge transport: Effect of dielectric surface energy and thermal annealing. *Phys. Rev. B: Condens. Matter Mater. Phys.* **2008**, *78*, 125319.
(20) McCulloch, I.; Heeney, M.; Chabinyc, M. L.; DeLongchamp, D.; Kline, R. J.; Cölle, M.; Duffy, W.; Fischer, D.; Gundlach, D.; Hamadani, B.; Hamilton, R.; Richter, L.; Salleo, A.; Shkunov, M.; Sparrowe, D.; Tierney, S.; Zhang, W. Semiconducting Thienothiophene Copolymers: Design, Synthesis, Morphology, and Performance in Thin-Film Organic Transistors. *Adv. Mater.* **2009**, *21*, 1091−1109.
(21) Goh, C.; Kline, R. J.; McGehee, M. D.; Kadnikova, E. N.; Frechet, J. M. J. Molecular-weight-dependent mobilities in regioregular poly(3-hexyl-thiophene) diodes. *Appl. Phys. Lett.* **2005**, *86*, 122110.
(22) Goh, C. T.; Kline, R. J.; McGehee, M. D.; Kadnikova, E. N.; Liu, J. S.; Frechet, J. M. J. Molecular weight dependent mobilities in regioregular poly(3-hexyl-thiophene) diodes and transistors. *Abstr. Pap. Am. Chem. Soc.* **2004**, *227*, U425−U425.
(23) Cao, Y.; Smith, P.; Heeger, A. J. Mechanical and electrical properties of polyacetylene films oriented by tensile drawing. *Polymer* **1991**, *32*, 1210−1218.
(24) Cao, Y.; Smith, P.; Heeger, A. J. Mechanical and electrical properties of highly oriented polyacetylene films. *Synth. Met.* **1991**, *41*, 181−184.
(25) Kline, R. J.; McGehee, M. D.; Kadnikova, E. N.; Liu, J. S.; Frechet, J. M. J. Controlling the field-effect mobility of regioregular polythiophene by changing the molecular weight. *Adv. Mater.* **2003**, *15*, 1519−1523.
(26) Kline, R. J.; McGehee, M. D.; Kadnikova, E. N.; Liu, J. S.; Frechet, J. M. J.; Toney, M. F. Dependence of regioregular poly(3-hexylthiophene) film morphology and field-effect mobility on molecular weight. *Macromolecules* **2005**, *38*, 3312−3319.
(27) Vakhshouri, K.; Gomez, E. D. Effect of Crystallization Kinetics on Microstructure and Charge Transport of Polythiophenes. *Macromol. Rapid Commun.* **2012**, *33*, 2133−2137.
(28) Mishra, S. P.; Deopura, B. L. Tie chains and modulus of nylon 6 fibers. *J. Appl. Polym. Sci.* **1982**, *27*, 3211−3218.
(29) Patel, S. K.; Malone, S.; Cohen, C.; Gillmor, J. R.; Colby, R. H. Elastic modulus and equilibrium swelling of poly(dimethylsiloxane) networks. *Macromolecules* **1992**, *25*, 5241−5251.
(30) Khang, D.-Y.; Rogers, J. A.; Lee, H. H. Mechanical Buckling: Mechanics, Metrology, and Stretchable Electronics. *Adv. Funct. Mater.* **2009**, *19*, 1526−1536.
(31) Li, F.; Lania, K.; Wang, X.; Xue, G.; Winter, H. H. Steric effects on the rheology of nanocomposite gels of organoclay in dicarboxyl-terminated polybutadiene. *Soft Matter* **2010**, *6*, 2442−2448.
(32) Moulton, J.; Smith, P. Electrical and mechanical properties of oriented poly(3-alkylthiophenes): 2. Effect of side-chain length. *Polymer* **1992**, *33*, 2340−2347.
(33) Stafford, C. M.; Harrison, C.; Beers, K. L.; Karim, A.; Amis, E. J.; VanLandingham, M. R.; Kim, H.-C.; Volksen, W.; Miller, R. D.; Simonyi, E. E. A buckling-based metrology for measuring the elastic moduli of polymeric thin films. *Nat. Mater.* **2004**, *3*, 545−550.
(34) Stafford, C. M.; Vogt, B. D.; Harrison, C.; Julthongpiput, D.; Huang, R. Elastic Moduli of Ultrathin Amorphous Polymer Films. *Macromolecules* **2006**, *39*, 5095−5099.
(35) Crosby, A. J.; Lee, J. Y. Polymer Nanocomposites: The "Nano" Effect on Mechanical Properties. *Polym. Rev.* **2007**, *47*, 217−229.
(36) Awartani, O. M.; Zhao, B.; Currie, T.; Kline, R. J.; Zikry, M. A.; O'Connor, B. T. Anisotropic Elastic Modulus of Oriented Regioregular Poly(3-hexylthiophene) Films. *Macromolecules* **2016**, *49*, 327−333.
(37) O'Connor, B.; Chan, E. P.; Chan, C.; Conrad, B. R.; Richter, L. J.; Kline, R. J.; Heeney, M.; McCulloch, I.; Soles, C. L.; DeLongchamp, D. M. Correlations between Mechanical and Electrical Properties of Polythiophenes. *ACS Nano* **2010**, *4*, 7538−7544.
(38) Chabinyc, M. L.; Toney, M. F.; Kline, R. J.; McCulloch, I.; Heeney, M. X-ray Scattering Study of Thin Films of Poly(2,5-bis(3-alkylthiophen-2-yl)thieno[3,2-b]thiophene). *J. Am. Chem. Soc.* **2007**, *129*, 3226−3237.
(39) Kline, R. J.; DeLongchamp, D. M.; Fischer, D. A.; Lin, E. K.; Richter, L. J.; Chabinyc, M. L.; Toney, M. F.; Heeney, M.; McCulloch, I. Critical Role of Side-Chain Attachment Density on the Order and Device Performance of Polythiophenes. *Macromolecules* **2007**, *40*, 7960−7965.
(40) McCulloch, I.; Heeney, M.; Bailey, C.; Genevicius, K.; Macdonald, I.; Shkunov, M.; Sparrowe, D.; Tierney, S.; Wagner, R.; Zhang, W. M.; Chabinyc, M. L.; Kline, R. J.; McGehee, M. D.; Toney, M. F. Liquid-crystalline semiconducting polymers with high charge-carrier mobility. *Nat. Mater.* **2006**, *5*, 328−333.
(41) Li, S. P.; Newsome, C. J.; Russell, D. M.; Kugler, T.; Ishida, M.; Shimoda, T. Friction transfer deposition of ordered conjugated polymer nanowires and transistor fabrication. *Appl. Phys. Lett.* **2005**, *87*, 062101.
(42) Sirringhaus, H.; Wilson, R. J.; Friend, R. H.; Inbasekaran, M.; Wu, W.; Woo, E. P.; Grell, M.; Bradley, D. D. C. Mobility enhancement in conjugated polymer field-effect transistors through chain alignment in a liquid-crystalline phase. *Appl. Phys. Lett.* **2000**, *77*, 406−408.
(43) Joseph Kline, R.; McGehee, M. D.; Toney, M. F. Highly oriented crystals at the buried interface in polythiophene thin-film transistors. *Nat. Mater.* **2006**, *5*, 222−228.
(44) Collins, B. A.; Cochran, J. E.; Yan, H.; Gann, E.; Hub, C.; Fink, R.; Wang, C.; Schuettfort, T.; McNeill, C. R.; Chabinyc, M. L.; Ade, H. Polarized X-ray scattering reveals non-crystalline orientational ordering in organic films. *Nat. Mater.* **2012**, *11*, 536−543.
(45) Certain commercial equipment and materials are identified in this paper in order to specify adequately the experimental procedure. In no case does such identification imply recommendations by the National Institute of Standards and Technology nor does it imply that

DOI: 10.1021/acs.macromol.6b01086
Macromolecules 2016, 49, 7359−7369

the material or equipment identified is necessarily the best available for this purpose.
(46) Smith, B. H.; Clark, M. B.; Kuang, H.; Grieco, C.; Larsen, A. V.; Zhu, C.; Wang, C.; Hexemer, A.; Asbury, J. B.; Janik, M. J.; Gomez, E. D. Controlling Polymorphism in Poly(3-Hexylthiophene) through Addition of Ferrocene for Enhanced Charge Mobilities in Thin-Film Transistors. *Adv. Funct. Mater.* **2015**, *25*, 542−551.
(47) Zen, A.; Pflaum, J.; Hirschmann, S.; Zhuang, W.; Jaiser, F.; Asawapirom, U.; Rabe, J. P.; Scherf, U.; Neher, D. Effect of Molecular Weight and Annealing of Poly(3-hexylthiophene)s on the Performance of Organic Field-Effect Transistors. *Adv. Funct. Mater.* **2004**, *14*, 757−764.
(48) Cho, S.; Lee, K.; Yuen, J.; Wang, G.; Moses, D.; Heeger, A. J.; Surin, M.; Lazzaroni, R. Thermal annealing-induced enhancement of the field-effect mobility of regioregular poly(3-hexylthiophene) films. *J. Appl. Phys.* **2006**, *100*, 114503.
(49) Baker, J. L.; Jimison, L. H.; Mannsfeld, S.; Volkman, S.; Yin, S.; Subramanian, V.; Salleo, A.; Alivisatos, A. P.; Toney, M. F. Quantification of Thin Film Crystallographic Orientation Using X-ray Diffraction with an Area Detector. *Langmuir* **2010**, *26*, 9146−9151.
(50) Tanase, C.; Blom, P. W. M.; de Leeuw, D. M.; Meijer, E. J. Charge carrier density dependence of the hole mobility in poly(p-phenylene vinylene). *physica status solidi (a)* **2004**, *201*, 1236−1245.
(51) Shehu, A.; Quiroga, S. D.; D'Angelo, P.; Albonetti, C.; Borgatti, F.; Murgia, M.; Scorzoni, A.; Stoliar, P.; Biscarini, F. Layered Distribution of Charge Carriers in Organic Thin Film Transistors. *Phys. Rev. Lett.* **2010**, *104*, 246602.
(52) Dinelli, F.; Murgia, M.; Levy, P.; Cavallini, M.; Biscarini, F.; de Leeuw, D. M. Spatially correlated charge transport in organic thin film transistors. *Phys. Rev. Lett.* **2004**, *92*, 116802.
(53) Kline, R. J.; McGehee, M. D.; Toney, M. F. Highly oriented crystals at the buried interface in polythiophene thin-film transistors. *Nat. Mater.* **2006**, *5*, 222−228.
(54) Sirringhaus, H. Device physics of Solution-processed organic field-effect transistors. *Adv. Mater.* **2005**, *17*, 2411−2425.
(55) Nelson, S. F.; Lin, Y.-Y.; Gundlach, D. J.; Jackson, T. N. Temperature-independent transport in high-mobility pentacene transistors. *Appl. Phys. Lett.* **1998**, *72*, 1854−1856.
(56) Bjorklund, T. G.; Lim, S.-H.; Bardeen, C. J. The optical spectroscopy of poly(p-phenylene vinylene)/polyvinyl alcohol blends: from aggregates to isolated chromophores. *Synth. Met.* **2004**, *142*, 195−200.
(57) Collison, C. J.; Rothberg, L. J.; Treemaneekarn, V.; Li, Y. Conformational Effects on the Photophysics of Conjugated Polymers: A Two Species Model for MEH−PPV Spectroscopy and Dynamics. *Macromolecules* **2001**, *34*, 2346−2352.
(58) Ho, P. K. H.; Kim, J.-S.; Tessler, N.; Friend, R. H. Photoluminescence of poly(p-phenylenevinylene)−silica nanocomposites: Evidence for dual emission by Franck−Condon analysis. *J. Chem. Phys.* **2001**, *115*, 2709−2720.
(59) Spano, F. C. Modeling disorder in polymer aggregates: The optical spectroscopy of regioregular poly(3-hexylthiophene) thin films. *J. Chem. Phys.* **2005**, *122*, 234701.
(60) Brown, P. J.; Thomas, D. S.; Köhler, A.; Wilson, J. S.; Kim, J.-S.; Ramsdale, C. M.; Sirringhaus, H.; Friend, R. H. Effect of interchain interactions on the absorption and emission of poly(3-hexylthiophene). *Phys. Rev. B: Condens. Matter Mater. Phys.* **2003**, *67*, 064203.
(61) Niles, E. T.; Roehling, J. D.; Yamagata, H.; Wise, A. J.; Spano, F. C.; Moulé, A. J.; Grey, J. K. J-Aggregate Behavior in Poly-3-hexylthiophene Nanofibers. *J. Phys. Chem. Lett.* **2012**, *3*, 259−263.
(62) Roehling, J. D.; Arslan, I.; Moule, A. J. Controlling microstructure in poly(3-hexylthiophene) nanofibers. *J. Mater. Chem.* **2012**, *22*, 2498−2506.
(63) Spano, F. C.; Clark, J.; Silva, C.; Friend, R. H. Determining exciton coherence from the photoluminescence spectral line shape in poly(3-hexylthiophene) thin films. *J. Chem. Phys.* **2009**, *130*, 074904.
(64) Manas, E. S.; Spano, F. C. Absorption and spontaneous emission in aggregates of conjugated polymers. *J. Chem. Phys.* **1998**, *109*, 8087−8101.
(65) Spano, F. C. Absorption in regio-regular poly(3-hexyl)thiophene thin films: Fermi resonances, interband coupling and disorder. *Chem. Phys.* **2006**, *325*, 22−35.
(66) Beljonne, D.; Cornil, J.; Silbey, R.; Millie, P.; Bredas, J. L. Interchain interactions in conjugated materials: The exciton model versus the supermolecular approach. *J. Chem. Phys.* **2000**, *112*, 4749−4758.
(67) Cornil, J.; dos Santos, D. A.; Crispin, X.; Silbey, R.; Brédas, J. L. Influence of Interchain Interactions on the Absorption and Luminescence of Conjugated Oligomers and Polymers: A Quantum-Chemical Characterization. *J. Am. Chem. Soc.* **1998**, *120*, 1289−1299.
(68) Chang, J.-F.; Clark, J.; Zhao, N.; Sirringhaus, H.; Breiby, D. W.; Andreasen, J. W.; Nielsen, M. M.; Giles, M.; Heeney, M.; McCulloch, I. Molecular-weight dependence of interchain polaron delocalization and exciton bandwidth in high-mobility conjugated polymers. *Phys. Rev. B: Condens. Matter Mater. Phys.* **2006**, *74*, 115318.
(69) Clark, J.; Chang, J.-F.; Spano, F. C.; Friend, R. H.; Silva, C. Determining exciton bandwidth and film microstructure in polythiophene films using linear absorption spectroscopy. *Appl. Phys. Lett.* **2009**, *94*, 163306.
(70) Turner, S. T.; Pingel, P.; Steyrleuthner, R.; Crossland, E. J. W.; Ludwigs, S.; Neher, D. Quantitative Analysis of Bulk Heterojunction Films Using Linear Absorption Spectroscopy and Solar Cell Performance. *Adv. Funct. Mater.* **2011**, *21*, 4640−4652.
(71) Ade, H.; Hsiao, B. X-ray Linear Dichroism Microscopy. *Science* **1993**, *262*, 1427−1429.
(72) Ade, H.; Toledo-Crow, R.; Vaez-Iravani, M.; Spontak, R. J. Observation of Polymer Birefringence in Near-Field Optical Microscopy. *Langmuir* **1996**, *12*, 231−234.
(73) Bräuer, B.; Virkar, A.; Mannsfeld, S. C. B.; Bernstein, D. P.; Kukreja, R.; Chou, K. W.; Tyliszczak, T.; Bao, Z.; Acremann, Y. X-ray Microscopy Imaging of the Grain Orientation in a Pentacene Field-Effect Transistor. *Chem. Mater.* **2010**, *22*, 3693−3697.
(74) Hub, C.; Burkhardt, M.; Halik, M.; Tzvetkov, G.; Fink, R. In situ STXM investigations of pentacene-based OFETs during operation. *J. Mater. Chem.* **2010**, *20*, 4884−4887.
(75) McNeill, C. R. Imaging the domain structure of organic semiconductor films. *J. Polym. Sci., Part B: Polym. Phys.* **2011**, *49*, 909−919.
(76) Zhang, X.; Hudson, S. D.; DeLongchamp, D. M.; Gundlach, D. J.; Heeney, M.; McCulloch, I. In-Plane Liquid Crystalline Texture of High-Performance Thienothiophene Copolymer Thin Films. *Adv. Funct. Mater.* **2010**, *20*, 4098−4106.
(77) McCulloch, B.; Ho, V.; Hoarfrost, M.; Stanley, C.; Do, C.; Heller, W. T.; Segalman, R. A. Polymer Chain Shape of Poly(3-alkylthiophenes) in Solution Using Small-Angle Neutron Scattering. *Macromolecules* **2013**, *46*, 1899−1907.
(78) Higgins, J. S.; Benoit, H. C. *Polymers and Neutron Scattering*; Oxford Series on Neutron Scattering in Condensed Matter; Lovesey, S. W., Mitchell, E. W., Eds.; Oxford University Press: New York, 1994.
(79) Zhang, W.; Gomez, E. D.; Milner, S. T. Predicting Nematic Phases of Semiflexible Polymers. *Macromolecules* **2015**, *48*, 1454−1462.
(80) Zhang, W.; Gomez, E. D.; Milner, S. T. Predicting Chain Dimensions of Semiflexible Polymers from Dihedral Potentials. *Macromolecules* **2014**, *47*, 6453−6461.
(81) Yang, H. C.; Shin, T. J.; Yang, L.; Cho, K.; Ryu, C. Y.; Bao, Z. N. Effect of mesoscale crystalline structure on the field-effect mobility of regioregular poly(3-hexyl thiophene) in thin-film transistors. *Adv. Funct. Mater.* **2005**, *15*, 671−676.
(82) Vakhshouri, K.; Kozub, D. R.; Wang, C.; Salleo, A.; Gomez, E. D. Effect of Miscibility and Percolation on Electron Transport in Amorphous Poly(3-Hexylthiophene)/Phenyl-C61-Butyric Acid Methyl Ester Blends. *Phys. Rev. Lett.* **2012**, *108*, 026601.
(83) Kozub, D. R.; Vakhshouri, K.; Orme, L. M.; Wang, C.; Hexemer, A.; Gomez, E. D. Polymer Crystallization of Partially Miscible Polythiophene/Fullerene Mixtures Controls Morphology. *Macromolecules* **2011**, *44*, 5722−5726.

DOI: 10.1021/acs.macromol.6b01086
Macromolecules 2016, 49, 7359−7369

(84) Vakhshouri, K.; Kesava, S. V.; Kozub, D. R.; Gomez, E. D. Characterization of the mesoscopic structure in the photoactive layer of organic solar cells: A focused review. *Mater. Lett.* **2013**, *90*, 97−102.
(85) Mao, Z.; Vakhshouri, K.; Jaye, C.; Fischer, D. A.; Fernando, R.; DeLongchamp, D. M.; Gomez, E. D.; Sauvé, G. Synthesis of Perfluoroalkyl End-Functionalized Poly(3-hexylthiophene) and the Effect of Fluorinated End Groups on Solar Cell Performance. *Macromolecules* **2013**, *46*, 103−112.
(86) Mach, P.; Pindak, R.; Levelut, A. M.; Barois, P.; Nguyen, H. T.; Baltes, H.; Hird, M.; Toyne, K.; Seed, A.; Goodby, J. W.; Huang, C. C.; Furenlid, L. Structures of chiral smectic-C mesophases revealed by polarization-analyzed resonant x-ray scattering. *Phys. Rev. E: Stat. Phys., Plasmas, Fluids, Relat. Interdiscip. Top.* **1999**, *60*, 6793−6802.
(87) Mezger, M.; Jérôme, B.; Kortright, J. B.; Valvidares, M.; Gullikson, E. M.; Giglia, A.; Mahne, N.; Nannarone, S. Molecular orientation in soft matter thin films studied by resonant soft x-ray reflectivity. *Phys. Rev. B: Condens. Matter Mater. Phys.* **2011**, *83*, 155406.
(88) Rivnay, J.; Noriega, R.; Kline, R. J.; Salleo, A.; Toney, M. F. Quantitative analysis of lattice disorder and crystallite size in organic semiconductor thin films. *Phys. Rev. B: Condens. Matter Mater. Phys.* **2011**, *84*, 045203.
(89) Seguela, R. Critical review of the molecular topology of semicrystalline polymers: The origin and assessment of intercrystalline tie molecules and chain entanglements. *J. Polym. Sci., Part B: Polym. Phys.* **2005**, *43*, 1729−1748.
(90) Seguela, R.; Rietsch, F. Molecular topology in ethylene copolymers studied by means of mechanical testing. *J. Mater. Sci.* **1988**, *23*, 415−421.
(91) Hong, K.; Rastogi, A.; Strobl, G. A Model Treating Tensile Deformation of Semicrystalline Polymers: Quasi-Static Stress−Strain Relationship and Viscous Stress Determined for a Sample of Polyethylene. *Macromolecules* **2004**, *37*, 10165−10173.
(92) Patel, R. M.; Sehanobish, K.; Jain, P.; Chum, S. P.; Knight, G. W. Theoretical prediction of tie-chain concentration and its characterization using postyield response. *J. Appl. Polym. Sci.* **1996**, *60*, 749−758.
(93) Huang, Y.-L.; Brown, N. Dependence of slow crack growth in polyethylene on butyl branch density: Morphology and theory. *J. Polym. Sci., Part B: Polym. Phys.* **1991**, *29*, 129−137.
(94) Groenewold, J. Wrinkling of plates coupled with soft elastic media. *Phys. A* **2001**, *298*, 32−45.
(95) Huang, Z. Y.; Hong, W.; Suo, Z. Nonlinear analyses of wrinkles in a film bonded to a compliant substrate. *J. Mech. Phys. Solids* **2005**, *53*, 2101−2118.
(96) Do, K.; Huang, D. M.; Faller, R.; Moule, A. J. A comparative MD study of the local structure of polymer semiconductors P3HT and PBTTT. *Phys. Chem. Chem. Phys.* **2010**, *12*, 14735−14739.
(97) Hu, Z.; Liu, J.; Simón-Bower, L.; Zhai, L.; Gesquiere, A. J. Influence of Backbone Rigidness on Single Chain Conformation of Thiophene-Based Conjugated Polymers. *J. Phys. Chem. B* **2012**, *117*, 4461.
(98) Arinstein, A.; Liu, Y.; Rafailovich, M.; Zussman, E. Shifting of the melting point for semi-crystalline polymer nanofibers. *EPL* **2011**, *93*, 46001.
(99) Xue, L.; Han, Y. Inhibition of dewetting of thin polymer films. *Prog. Mater. Sci.* **2012**, *57*, 947−979.

DOI: 10.1021/acs.macromol.6b01086
Macromolecules 2016, 49, 7359−7369